

Published in final edited form as:

*J Porphyr Phthalocyanines*. 2008 September 1; 12(9): 971–978. doi:10.1142/S1088424608000352.

## Probing the heme-thiolate oxygenase domain of inducible nitric oxide synthase with Ru(II) and Re(I) electron tunneling wires

Charlotte A. Whited, Wendy Belliston-Bittner, Alexander R. Dunn, Jay R. Winkler\*, and Harry B. Gray\*

Beckman Institute, California Institute of Technology, Pasadena, 91125, USA

### Abstract

Nitric oxide synthase (NOS) catalyzes the production of nitric oxide from L-arginine and dioxygen at a thiolate-ligated heme active site. Although many of the reaction intermediates are as yet unidentified, it is well established that the catalytic cycle begins with substrate binding and rate-limiting electron transfer to the heme. Here we show that Ru(II)-diimine and Re(I)-diimine electron tunneling wires trigger nanosecond photoreduction of the active-site heme in the enzyme. Very rapid generation of a reduced thiolate-ligated heme opens the way for direct observation of short-lived intermediates in the NOS reaction cycle.

### INTRODUCTION

Salvador Moncada and colleagues reported in 1987 that the molecule responsible for relaxation of blood vessels is nitric oxide (NO).<sup>1</sup> This publication marked the beginning of a new area of chemical and biological research, with thousands of articles published each year. Long known as a cytotoxic agent in pathological processes,<sup>2</sup> NO now is recognized as a key signaling molecule in the cardiovascular, immune, and nervous systems.<sup>3</sup>

Nitric oxide synthases (NOSs) are responsible for the production of NO in living systems.<sup>4</sup> The three (mammalian) isoforms of the enzyme are named for the tissues in which they are found: endothelial NOS (eNOS), neuronal (nNOS), and an inducible form found in macrophages (iNOS). The functions of eNOS and nNOS are regulated by calcium ions and a calmodulin linker, while the inducible isoform is calcium ion independent.<sup>5</sup> NOSs catalyze the oxidation of L-arginine (Arg) to L-citrulline in two turnovers, with N<sup>ω</sup>-hydroxy-L-arginine (NHA or ArgOH) as an enzyme-bound intermediate (the product of the first turnover).<sup>6</sup> The overall reaction is shown in Scheme 1.

All three isoforms are found as homodimers, each monomer consisting of an oxygenase and a reductase domain.<sup>8</sup> The reductase domain binds flavin adenine dinucleotide (FAD) and flavin mononucleotide (FMN), cofactors that shuttle electrons from nicotinamide adenine dinucleotide phosphate (NADPH),<sup>9</sup> the ultimate source of electrons for the reaction, to the oxygenase domain where substrate oxidation occurs. The oxygenase domain contains a thiolate-ligated heme (protoporphyrin IX, or P-IX) as in cytochromes P450 (P450) and (6R)–5,6,7,8-tetrahydrobiopterin (pterin, H<sub>4</sub>B).<sup>8</sup> NO is produced when this domain is supplied with electrons from the reductase domain to activate dioxygen,<sup>10</sup> and in the presence of fully reduced pterin cofactor.<sup>11, 12</sup> Although structural characterization of full-length NOS has not been reported to date, structures of individual domains are known.<sup>13, 14</sup>

\*Correspondence to: J. R. Winkler; winklerj@caltech.edu; H. B. Gray; hbgray@caltech.edu.

The mechanism of NO production is incompletely understood.<sup>15</sup> The resting state of the enzyme is a six-coordinate ferric heme with a water molecule occupying the sixth ligand position (four positions are occupied by N donors from the porphyrin, one by a sulfur atom from an axial cysteine, Cys194).<sup>16</sup> Although neither Arg nor ArgOH ligates the heme, substrate binding shifts both the Soret absorption maximum and the heme spin state.<sup>7, 17</sup> One-electron reduction of the NOS:substrate complex gives a five-coordinate ferrous that readily binds dioxygen, forming a ferrous-oxy species (equivalent to ferric superoxide),<sup>8</sup> the last observed intermediate in the catalytic cycle.<sup>8, 18</sup>

The role of pterin has been extensively investigated.<sup>11, 16, 19</sup> This molecule binds in a pocket alongside the heme, forming hydrogen bonds with a P-IX carboxylate, thereby coupling it to the active site.<sup>13</sup> It is known that a pterin-based radical forms and is reduced during the catalytic cycle, as determined by analysis of results from rapid-freeze EPR experiments.<sup>12, 20</sup> Turnover has never been observed without fully reduced pterin cofactor.<sup>21</sup>

The NOS reaction cycle bears many similarities to that of P450s. P450s contain thiolate-heme active sites and hydroxylate substrates via two-electron oxidation processes.<sup>22, 23</sup> The P450 cycle also begins with substrate binding followed by heme reduction, dioxygen binding, and another reduction step leading to the formation of a high-valent iron-oxo complex (Compound I) that hydroxylates the substrate (Scheme 2).<sup>23</sup> Separate enzymes serve as reductases for P450s, but substrate hydroxylation can be driven using external sources of electrons.<sup>24</sup> Owing to these similarities, the mechanism of the first turnover of NOS is postulated to be the same as that of P450s.<sup>25</sup> However, the second turnover, a three-electron oxidation, is thought to employ a unique mechanism.<sup>26</sup> It has been suggested that a protonated ferric hydroperoxide may act as the nucleophile in the second turnover<sup>18</sup> rather than Compound I, which is a ferryl P-IX radical cation.<sup>8</sup>

Steps in the mechanistic cycle borrowed from P450 are shown in Scheme 2. Although several intermediates in the P450 cycle already have been observed, there can be no doubt that “the hunt for an unambiguous experimental identification of the ephemeral active oxygen species will most certainly continue.”<sup>22</sup> If that is the case for P450, then we may conclude that work on the NOS catalytic cycle is just beginning.

A long-standing goal in our group is the development of methods to generate and observe high-valent iron-oxo complexes that are believed to play key roles as intermediates in the catalytic cycles of heme enzymes.<sup>27</sup> Direct observation during turnover would allow definitive identification of the active oxidant. Drawing on studies of similar enzymes and using EPR under cryogenic conditions and X-ray crystallography, investigators have amassed a large body of evidence that strongly indicates that Compound I (Scheme 2, the ferryl P-IX radical cation shown in red) is the active species.<sup>28</sup> The steps leading to formation of this highly reactive species are slow, making its observation problematic, as at best it is present in very low concentrations during catalysis.

We have investigated the redox photochemistry of two heme enzymes, microperoxidase-8 (MP-8, a heme octapeptide fragment of cytochrome *c*) and horseradish peroxidase (HRP).<sup>29</sup> Visible excitation of  $\text{Ru}(\text{bpy})_3^{2+}$  (bpy is 2,2'-bipyridine) in the presence of oxidative quenchers in solution generates a powerful Ru(III)-diimine oxidant, which reacts rapidly with P-IX to form the P-IX radical cation, which then oxidizes Fe(III) to give high-valent iron-oxo complexes of MP-8 and HRP.<sup>29, 30</sup> Attempts to generate high-valent hemes in P450s in reactions with uncomplexed photogenerated oxidants were not successful so we changed course, as discussed in the following section.

## CHANNEL-BINDING WIRES

Since 1999 we have developed sensitizer-linked electron tunneling wires that are able to deliver electrons and holes rapidly to and from deeply buried active sites of heme enzymes.<sup>31, 32</sup> Attaching the photosensitizer to the substrate promotes a close interaction between the two, and increases the probability of ET (Figure 1). A selection of such molecules developed for the oxygenase domain of iNOS is shown in Chart 1.

The dissociation constants of complexes that contain wires in the substrate channels of enzymes can be determined from analysis of shifts in Soret absorptions. Examples of these shifts in the case of iNOSoxy are shown in Figure 2.<sup>34</sup>

The wires luminesce upon 355 nm (Re(I)) or 480 nm (Ru(II)) excitation. The emission overlap with heme absorptions triggers Forster energy transfer (FET), which accounts for the steady-state emission quenching observed upon binding of wires to iNOSoxy (Figure 3).<sup>34</sup>

Transient absorption measurements demonstrate that these wires reduce iNOSoxy upon 355 or 480 nm excitation. Reduction is indicated by a bleach near 420 nm, corresponding to the disappearance of the six-coordinate Fe(III) resting state and the formation of a new species (with absorption near 445 nm) assigned to six-coordinate Fe(II). Difference spectra were constructed from single-wavelength transient absorption traces 80 ns after excitation of the protein-bound wire **7** (Figure 3, blue) and 3  $\mu$ s after excitation of protein-bound wire **5** (Figure 4, red).

Picosecond transient absorption measurements demonstrate rapid formation of Fe(II) in the presence of wires **5** and **7**. By pumping with 70 ps, 355 nm pulses and probing with 442 nm radiation from a continuous wave He:Cd laser, we obtained transient absorbance traces that document the formation of a ferrous heme on very short timescales (Figure 5). The traces were fit to a single exponential to give  $k_f = 7(3) \times 10^9 \text{ s}^{-1}$  for formation of Fe(II).

Although the demonstration of very rapid electron transfer to a heme active site represents a step toward the goal of observing high-valent intermediates, our electron delivering wires block access to substrate channels (Figure 6).<sup>33</sup> We have exploited this property of channel binders in the construction of highly selective amine oxidase inhibitors by manipulation of the linker elements of wire structures.<sup>35</sup>

## SURFACE-BINDING WIRES

We are investigating wires that bind on enzyme surfaces, as they are much less likely to impede substrate binding (Chart 2). The luminescence of wire **9** is quenched upon binding to iNOSoxy (Figure 7), and addition of channel binder **5** does not alter the decay rate.

Upon electronic excitation, surface binders **9–12** trigger ET without blocking substrate or cofactor binding, maintaining the potential for enzymatic turnover.

We have shown that **9** binds to iNOSoxy independently of substrate and pterin with a dissociation constant of  $< 1 \mu\text{M}$ .<sup>34</sup> Binding distant from the active site is demonstrated by the finding that a known channel binder does not displace **9** from the enzyme.<sup>34</sup> While the precise binding site has not been definitively established, FET measurements indicate that it may be in the hydrophobic pocket thought to be the docking site for the iNOS reductase domain.<sup>34, 37</sup> Experiments with  $\text{Ru}(\text{bpy})_3^{2+}$  show that the sensitizer alone does not bind to the enzyme, suggesting that the perfluorobiphenyl unit is largely responsible for the association of the wire with a hydrophobic iNOSoxy surface region.

Single-wavelength transient absorbance measurements with imidazole-bound iNOSoxy in the presence of one equivalent of **9**, 10 mM ascorbate, and saturated tetramethylphenylenediamine (TMPD) confirm that Fe(II) forms within 50 ns of excitation at 480 nm (Figure 9).<sup>38</sup> A difference spectrum constructed from the single-wavelength data at 2  $\mu$ s (Figure 10) shows the bleach of the imidazole-Fe(III) Soret absorption peak at 428 nm and the development of the imidazole-Fe(II) feature at 445 nm. Control experiments with Ru(bpy)<sub>3</sub><sup>2+</sup> demonstrate that the perfluorobiphenyl moiety of **9** is required for heme reduction. In the presence of Ru(bpy)<sub>3</sub><sup>2+</sup> and quenchers, transient absorbance traces show only the production of Ru(I).<sup>38</sup>

To estimate the specific rate of Fe(II) formation, \*Ru(II) contributions were subtracted from the transient absorbance data.<sup>38</sup> Representative traces are shown in Figure 11. The traces were fit to a single-exponential function to obtain  $k_{ET} = 2(1) \times 10^7 \text{ s}^{-1}$ .

This is a remarkably fast reduction given the estimated Ru-Fe distance of 20.2 Å<sup>34</sup> and the absence of a through-bond pathway to the heme. Given its slim profile, hydrophobicity, and potential to  $\pi$ -stack with aromatic residues, the perfluorobiphenyl moiety of **9** could penetrate into the protein interior, leaving open the possibility of a through-wire hopping mechanism.<sup>18</sup>

## CONCLUSIONS

We have developed a system in which the heme of inducible nitric oxide synthase can be photoreduced rapidly without interfering with substrate or cofactor binding. Employing flash-quench experiments with a surface-binding Ru-diimine wire in combination with reductive quenchers, we observed ET to the imidazole-bound heme of iNOSoxy fully seven orders of magnitude faster than the natural reduction. This finding represents an important step toward our goal of identifying reactive intermediates in the catalytic cycles of heme oxotransferases.

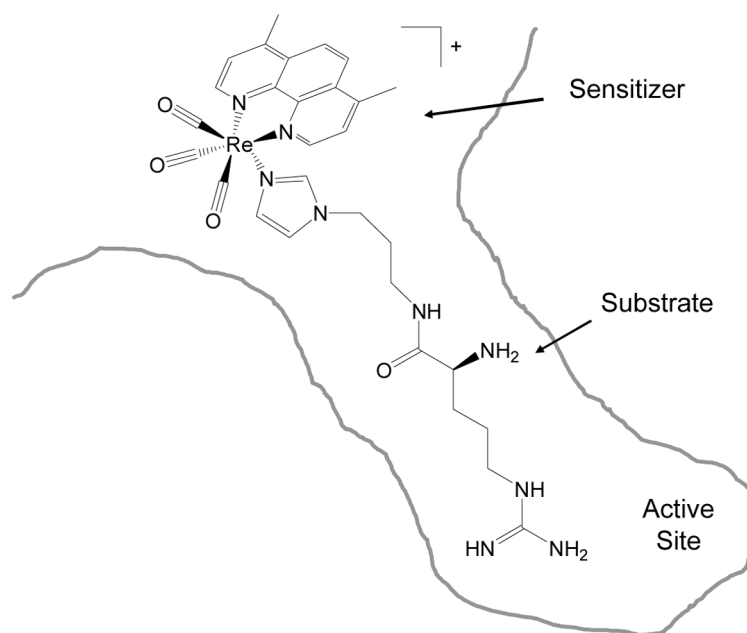
## Acknowledgments

Our work is supported by the NIH (DK19038 and GM070868 to HBG; GM068461 to JRW); the Ellison Medical Foundation (Senior Scholar Award in Aging to HBG); an NSF graduate fellowship (CAW); the Fannie and John Hertz Foundation (ARD); the Parsons Foundation (WBB); and the Arnold and Mabel Beckman Foundation.

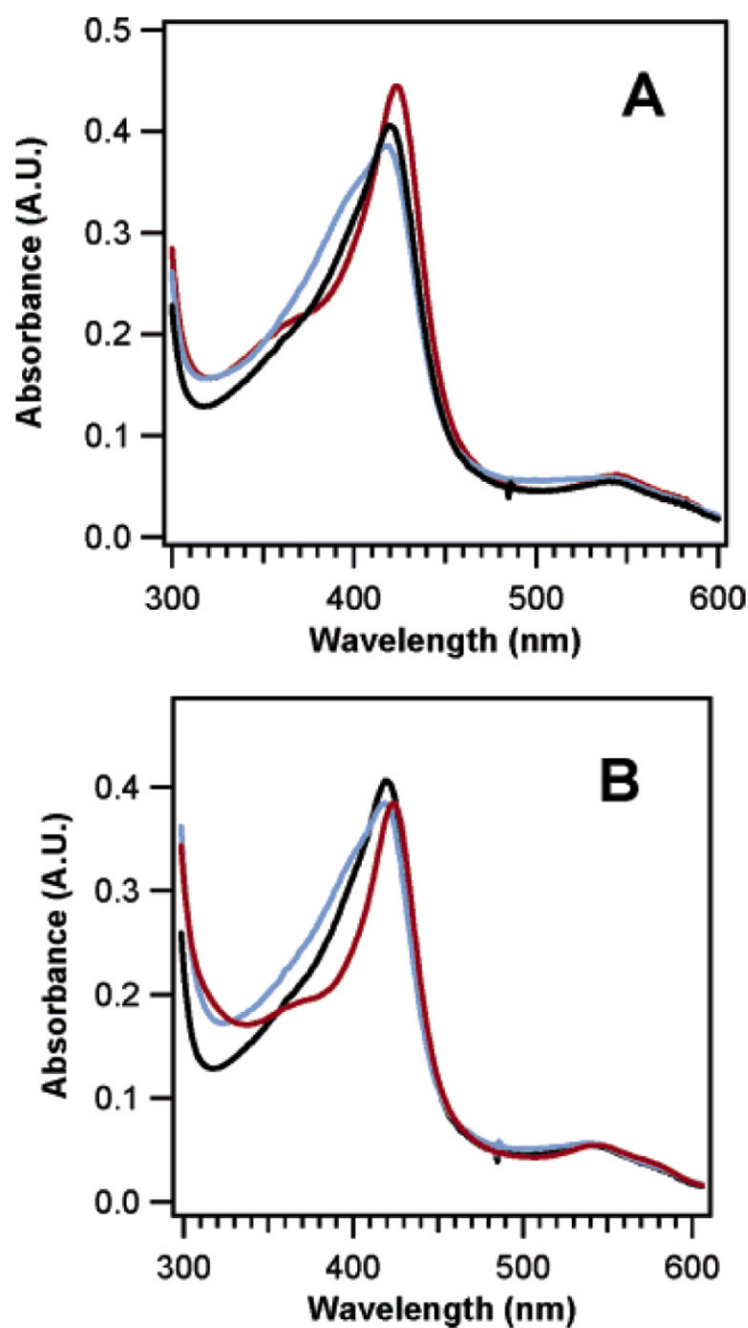
## References

- Palmer RMJ, Ferrige AG, Moncada S. Nature 1987;327:524–526. [PubMed: 3495737]
- Xie QW, Cho HJ, Calaycay J, Mumford RA, Swiderek KM, Lee TD, Ding AH, Troso T, Nathan C. Science 1992;256:225–228. [PubMed: 1373522]
- Sagami I, Sato Y, Noguchi T, Miyajima M. Coord Chem Rev 2002;226:179–186.
- Li HY, Igarashi J, Jamal J, Yang WP, Poulos TL. J Biol Inorg Chem 2006;11:753–768. [PubMed: 16804678]
- Stuehr DJ, Santolini J, Wang ZQ, Wei CC, Adak S. J Biol Chem 2004;279:36167–36170. [PubMed: 15133020]
- Marletta MA. J Biol Chem 1993;268:12231–12234. [PubMed: 7685338]
- Hurshman AR, Marletta MA. Biochemistry 1995;34:5627–5634. [PubMed: 7537092]
- Alderton WK, Cooper CE, Knowles RG. Biochem J 2001;357:593–695. [PubMed: 11463332]
- Stuehr DJ, Cho HJ, Kwon NS, Weise MF, Nathan CF. Proc Nat Acad Sci USA 1991;88:7773–7777. [PubMed: 1715579]
- Hurshman AR, Marletta MA. Biochemistry 2002;41:3439–3456. [PubMed: 11876653]
- Hevel JM, Marletta MA. Biochemistry 1992;31:7160–7165. [PubMed: 1379468]
- Hurshman AR, Krebs C, Edmondson DE, Huynh BH, Marletta MA. Biochemistry 1999;38:15689–15696. [PubMed: 10625434]

13. Crane BR, Arvai AS, Ghosh DK, Wu CQ, Getzoff ED, Stuehr DJ, Tainer JA. *Science* 1998;279:2121–2126. [PubMed: 9516116]
14. Garcin ED, Bruns CM, Lloyd SJ, Hosfield D, Tiso M, Stuehr DJ, Tainer JA, Getzoff ED. *J Biol Chem* 2004;279:37918–37927. [PubMed: 15208315]
15. Zhu Y, Silverman RB. *Biochemistry*. 2008
16. Presta A, Weber-Main AM, Stankovich MT, Stuehr DJ. *J Am Chem Soc* 1998;120:9460–9465.
17. Lippard, SJ.; Berg, JM. *Principles of Bioinorganic Chemistry*. Mill Valley, CA: University Science Books; 1994.
18. Belliston-Bittner W, Dunn AR, Nguyen YHL, Stuehr DJ, Winkler JR, Gray HB. *J Am Chem Soc* 2005;127:15907–15915. [PubMed: 16277534]
19. Wang ZQ, Wei CC, Santolini J, Panda K, Wang Q, Stuehr DJ. *Biochemistry* 2005;44:4676–4690. [PubMed: 15779894]
20. Wei CC, Wang ZQ, Hemann C, Hille R, Stuehr DJ. *J Biol Chem* 2003;278:46668–46673. [PubMed: 14504282]
21. Ghosh DK, Wu CQ, Pitters E, Moloney M, Werner ER, Mayer B, Stuehr DJ. *Biochemistry* 1997;36:10609–10619. [PubMed: 9271491]
22. Denisov IG, Makris TM, Sligar SG, Schlichting I. *Chem Rev* 2005;105:2253–2277. [PubMed: 15941214]
23. Meunier B, de Visser SP, Shaik S. *Chem Rev* 2004;104:3947–3980. [PubMed: 15352783]
24. Udit AK, Hill MG, Gray HB. *Langmuir* 2006;22:10854–10857. [PubMed: 17129070]
25. Udit AK, Belliston-Bittner W, Glazer EC, Le Nguyen YH, Gillan JM, Hill MG, Marletta MA, Goodin DB, Gray HB. *J Am Chem Soc* 2005;127:11212–11213. [PubMed: 16089428]
26. Martin NI, Woodward JJ, Winter MB, Beeson WT, Marletta MA. *J Am Chem Soc* 2007;129:12563–12570. [PubMed: 17892291]
27. Green MT, Dawson JH, Gray HB. *Science* 2004;304:1653–1656. [PubMed: 15192224]
28. Wang R, de Visser SP. *J Inorg Biochem* 2007;101:1464–1472. [PubMed: 17659781]
29. Berglund J, Pascher T, Winkler JR, Gray HB. *J Am Chem Soc* 1997;119:2464–2469.
30. Low DW, Winkler JR, Gray HB. *J Am Chem Soc* 1996;118:117–120.
31. Wilker JJ, Dmochowski IJ, Dawson JH, Winkler JR, Gray HB. *Angew Chem Int Edit* 1999;38:89–92.
32. Dmochowski IJ, Dunn AR, Wilker JJ, Crane BR, Green MT, Dawson JH, Sligar SG, Winkler JR, Gray HB. *Method Enzymol* 2002;357:120–133.
33. Nguyen, YHL. *Wiring Inducible Nitric Oxide Synthase*. Pasadena, CA: Department of Chemistry, California Institute of Technology; 2006.
34. Dunn AR, Belliston-Bittner W, Winkler JR, Getzoff ED, Stuehr DJ, Gray HB. *J Am Chem Soc* 2005;127:5169–5173. [PubMed: 15810851]
35. Langley DB, Brown DE, Cheruzel LE, Contakes SM, Duff AP, Hilmer KM, Dooley DM, Gray HB, Guss JM, Freeman HC. *J Am Chem Soc* 2008;130:8069–8079. [PubMed: 18507382]
36. Belliston-Bittner, W. *Ultrafast Photoreduction of Nitric Oxide Synthase by Electron Tunneling Wires*. Pasadena, CA: Chemistry, California Institute of Technology; 2005.
37. Garcin ED, Bruns CM, Lloyd SJ, Hosfield DJ, Tiso M, Gachhui R, Stuehr DJ, Tainer JA, Getzoff ED. *J Biol Chem* 2004;279:37918–37927. [PubMed: 15208315]
38. Belliston-Bittner W, Dunn AR, Winkler JR, Gray HB. 2008submitted



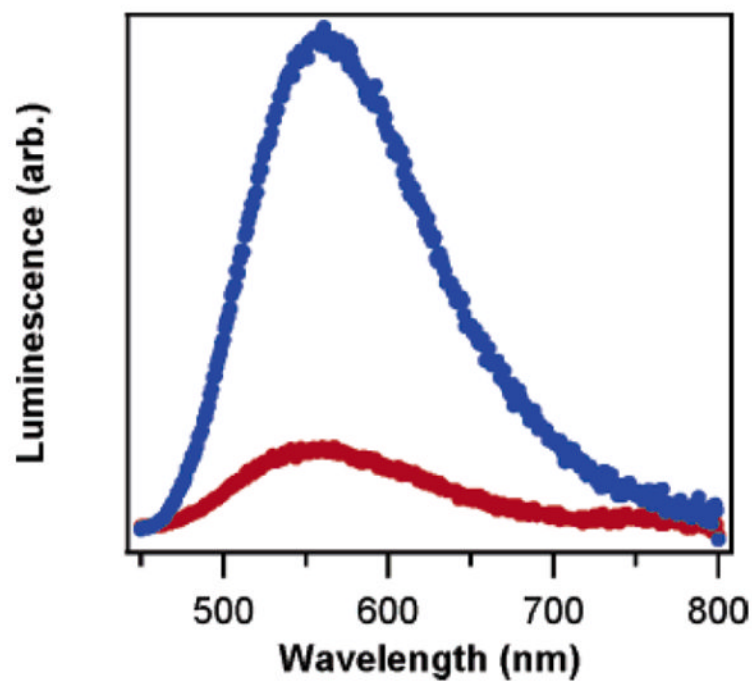
**Figure 1.**  
Substrates linked to sensitizers target active-site channels of enzymes.



**Figure 2.**

UV-visible absorption spectra of iNOSoxy: wire complexes. (A) iNOSoxy alone (5  $\mu$ M; black) and bound to 1 equivalent each of **5** (red) and **4** (blue). (B) iNOSoxy alone (5  $\mu$ M; black) and bound to 1 equivalent each of **7** (red) and **6** (blue).

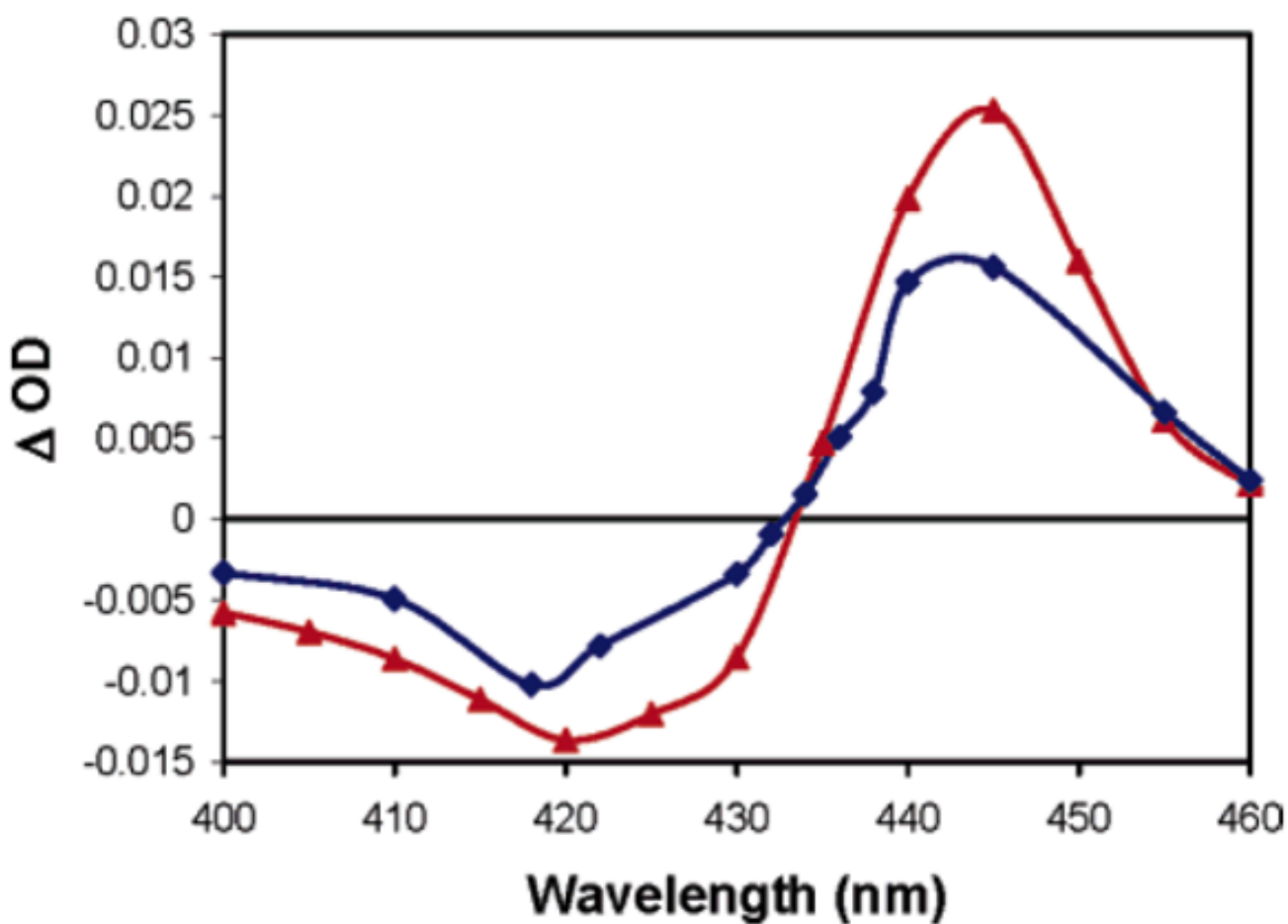




**Figure 3.**

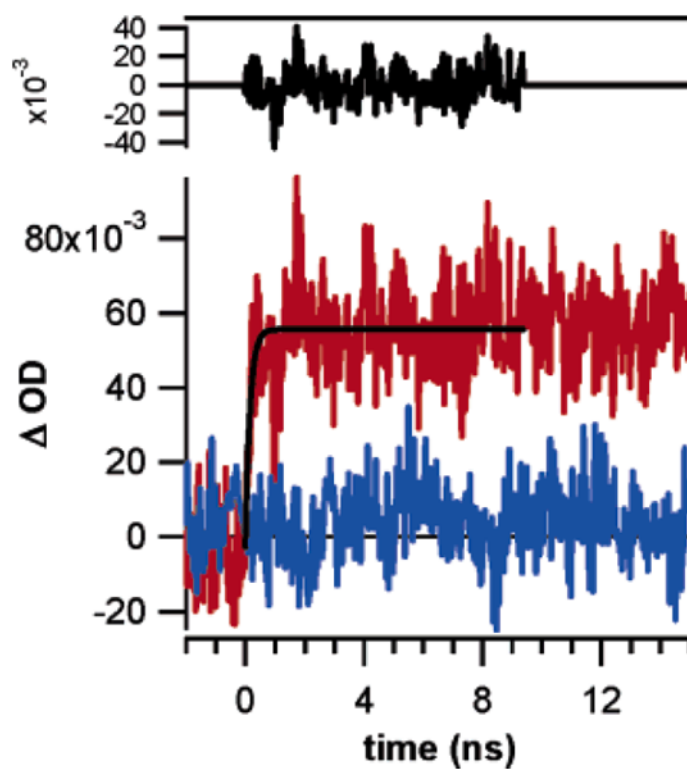
Steady-state luminescence spectra of **5** (2 μM; blue) and a 1:1 mixture of **5** and iNOS<sub>oxy</sub> (2 μM; red) with  $\lambda_{\text{ex}} = 355$  nm.





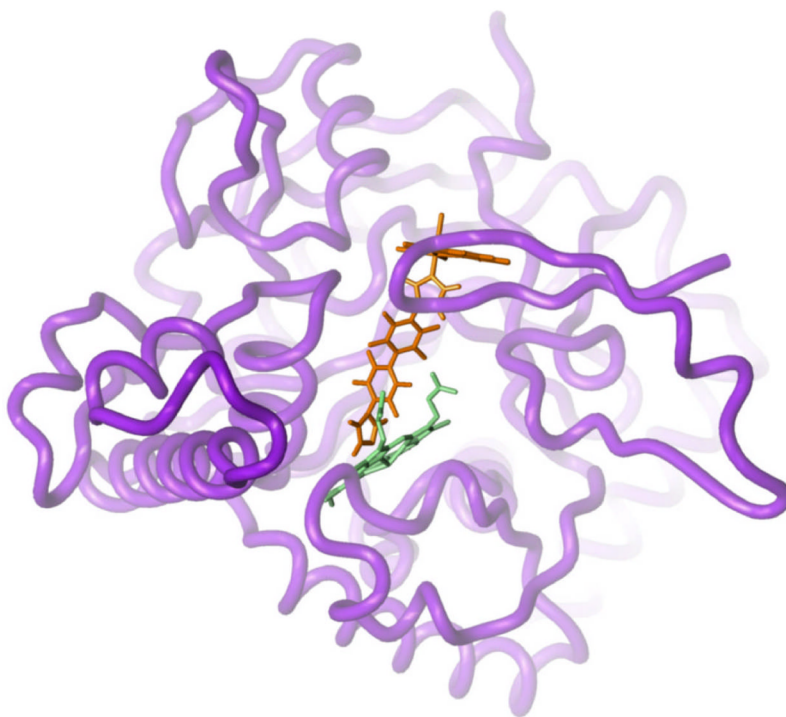
**Figure 4.**

Difference spectra of a 1:1 mixture of **7** and iNOSoxy (5  $\mu$ M, 80 ns after 355 nm excitation, blue squares) and a 1:1 mixture of **5** and iNOSoxy (11  $\mu$ M, 3  $\mu$ s after 355 nm excitation, red triangles) showing a bleach of a six-coordinate Fe(III) Soret (420 nm) and the appearance of a six-coordinate Fe(II) Soret (445 nm). Individual points were taken from single-wavelength transient absorption traces.

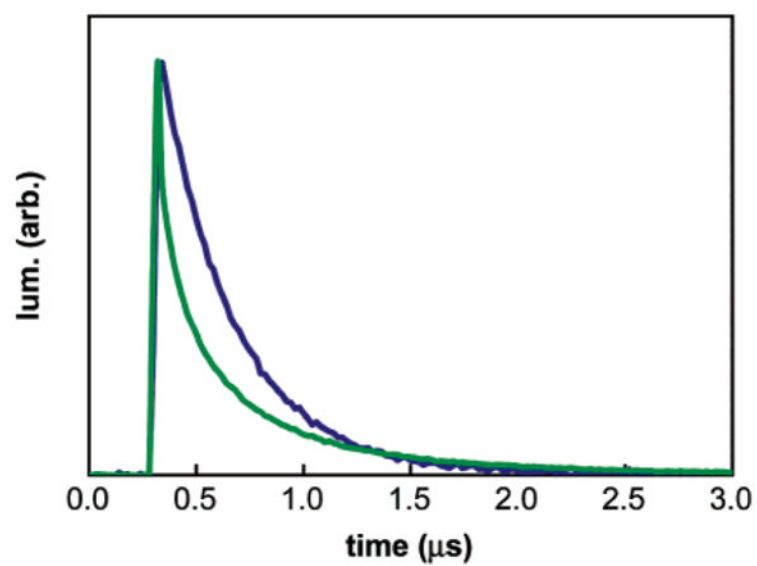


**Figure 5.**

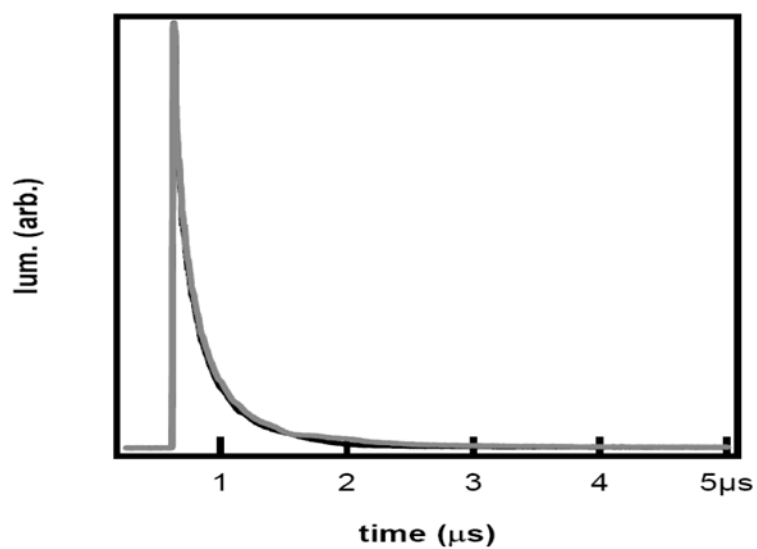
Transient absorbance at 442 nm of iNOSoxy alone (8  $\mu$ M, blue) and in the presence of excess **5** (red) with  $\lambda_{ex} = 355$  nm. The red trace shows the rapid formation of ferrous heme fit to one exponential ( $k_f = 7(3) \times 10^9 \text{ s}^{-1}$  black) with the residual shown above.



**Figure 6.** Structural model of Re-perfluorobiphenyl wire **5** in the substrate channel of iNOSoxy.<sup>36</sup>

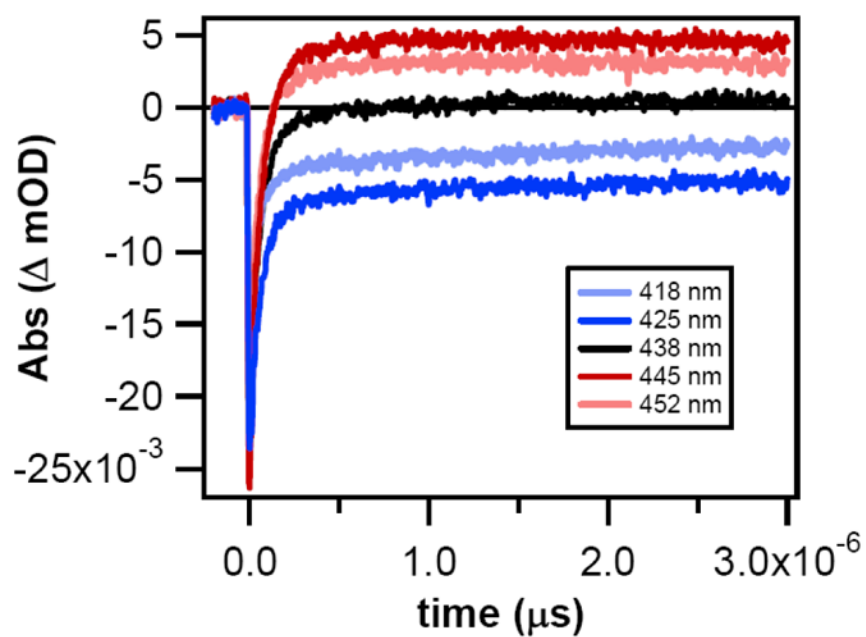


**Figure 7.** Transient decay data for **9** (blue) and a 1:1 mixture of **9** and iNOSoxy (1.8 μM; green). The fast component of the luminescence decay is assigned to the complex between **9** and iNOSoxy.

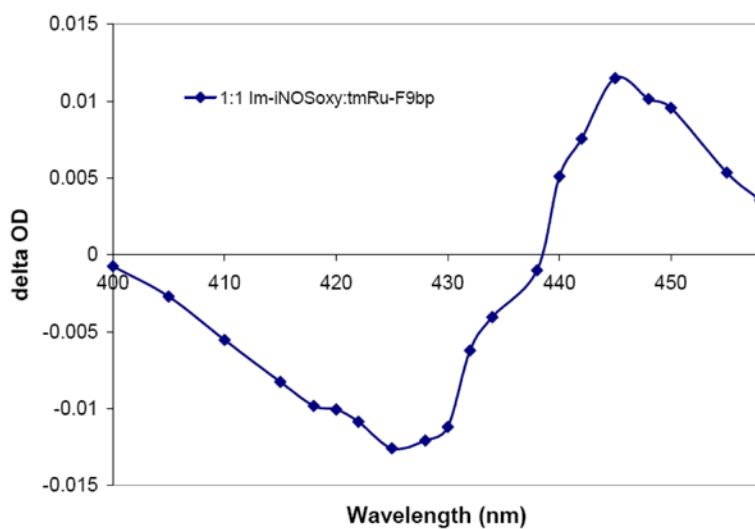


**Figure 8.**

Transient luminescence decay data for a 2:1 mixture of **9** with iNOSoxy (black) and a 2:1:1 mixture of **9**, **5**, and iNOSoxy (gray). In the second mixture, **5** was shown by UV-visible absorption spectroscopy to be bound in the active site. Since the luminescence decay of **9** was not disturbed by the binding of **5**, these traces indicate that **9** does not bind in the active-site channel.



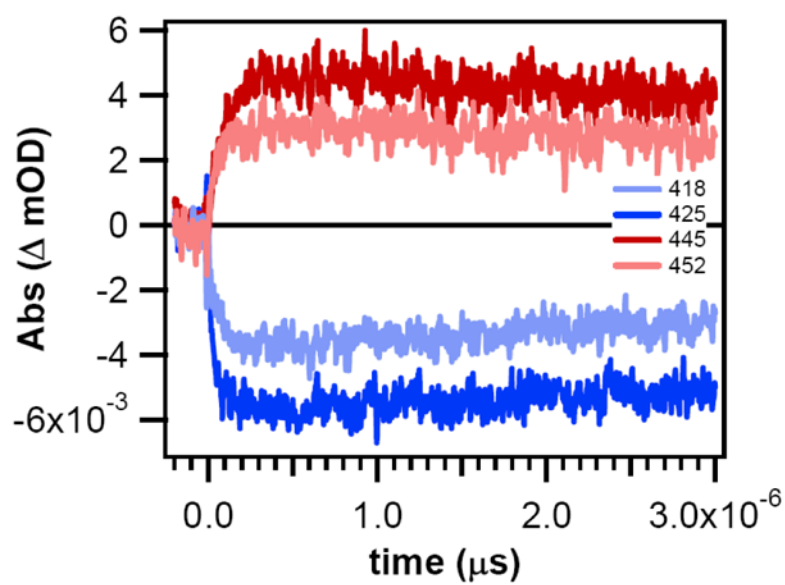
**Figure 9.** Transient absorbance of quenched imidazole-iNOSoxy bound to 1 equivalent of 9 (11  $\mu\text{M}$  with 10 mM ascorbate and saturated TMPD).  $\lambda_{\text{ex}} = 480 \text{ nm}$ .



**Figure 10.**

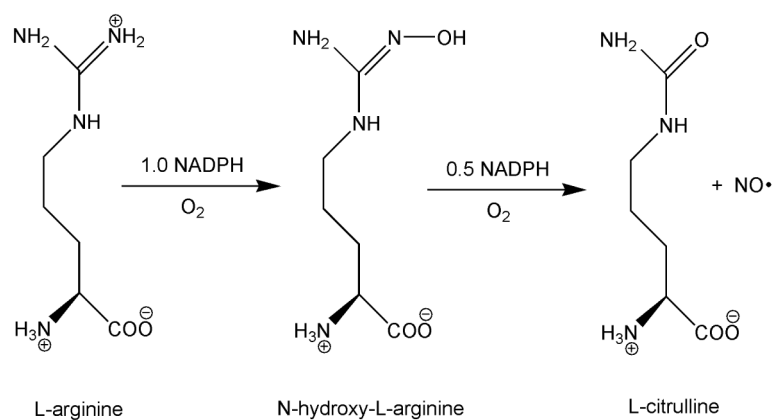
Transient absorbance of a 1:1 mixture of imidazole-iNOSoxy and 9 (22 μM with 10 mM ascorbate and saturated TMPD) showing a characteristic Fe(III/II) difference spectrum. Individual points were taken from single-wavelength transient absorbance traces, 2 μs after 480 nm excitation.



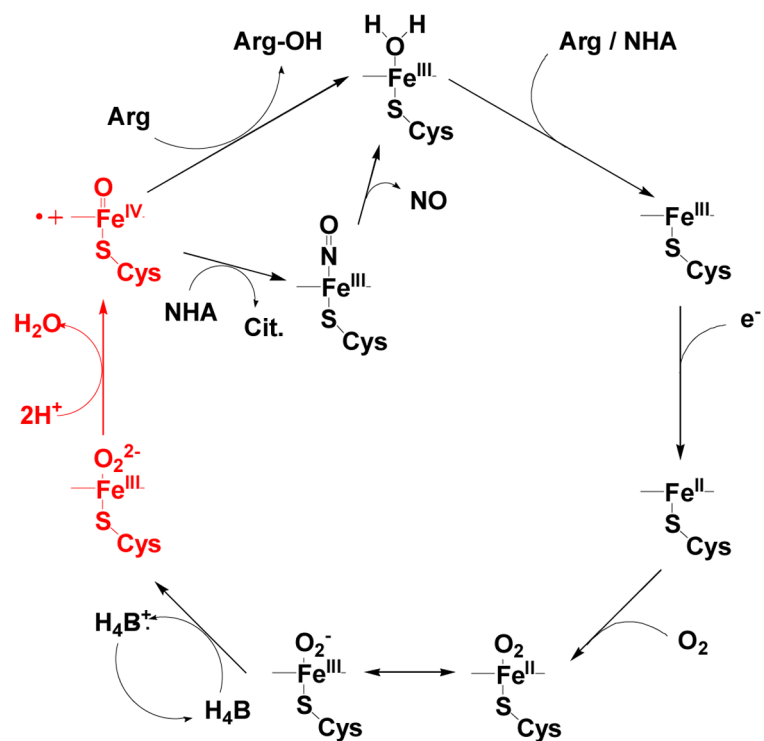


**Figure 11.**

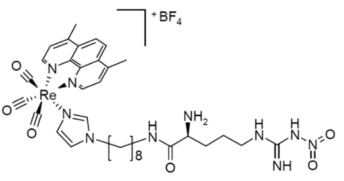
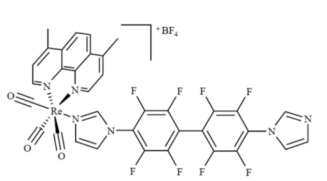
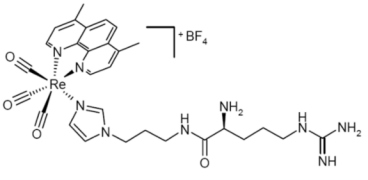
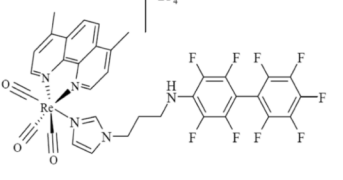
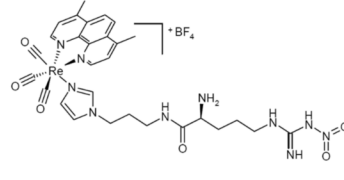
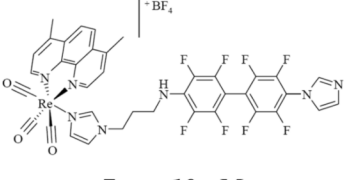
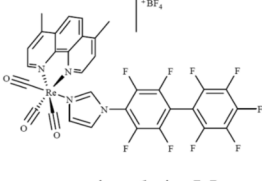
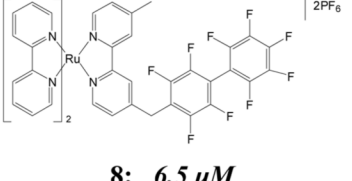
Transient absorbance of imidazole-iNOSoxy bound to 1 equivalent of 9 (11 μM with 10 mM ascorbate and saturated TMPD) corrected for absorbance due to \*Ru(II) to reveal  $k_{ET} = 2(1) \times 10^7 \text{ s}^{-1}$ .



**Scheme 1.**  
The five-electron oxidation of arginine to form NO and citrulline.<sup>7</sup>

**Scheme 2.**

Proposed NOS catalytic cycle; active-site intermediates that have not been observed are shown in red.

<i>Channel-Binding Wires</i>	
 <p><b>1: 3 <math>\mu</math>M</b></p>	 <p><b>5: 0.13 <math>\mu</math>M</b></p>
 <p><b>2: 2 <math>\mu</math>M</b></p>	 <p><b>6: &lt; 10 <math>\mu</math>M</b></p>
 <p><b>3: 7 <math>\mu</math>M</b></p>	 <p><b>7: &lt; 10 <math>\mu</math>M</b></p>
 <p><b>4: 1.4 <math>\mu</math>M</b></p>	 <p><b>8: 6.5 <math>\mu</math>M</b></p>

**Chart 1.**

Ru(II) and Re(I) electron tunneling wires bind to the oxygenase domain of murine inducible nitric oxide synthase (iNOSoxy).<sup>18, 33</sup>

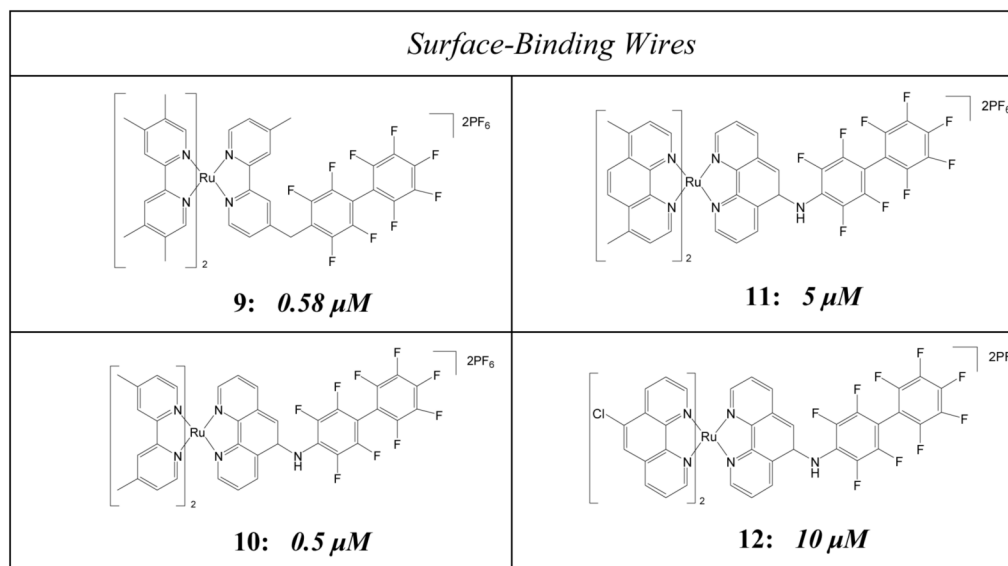


**Chart 2.**  
Four wires that bind on iNOSoxy surfaces.